Model Reduction for an Internally Damped n-Particle Chain In a Potential Well Under Polyharmonic Excitation

Attila Genda[1*], Alexander Fidlin[1] and Oleg Gendelman[2]

[1*]Institute of Engineering Mechanics, Karlsruhe Institute of Technology, Kaiserstr. 12, Karlsruhe, 76131, Germany.

[2]Faculty of Mechanical Engineering, Technion - Israel Institute of Technology, Haifa, 3200003, Israel.

*Corresponding author(s). E-mail(s): attila.genda@kit.edu;

Contributing authors: alexander.fidlin@kit.edu; ovgend@me.technion.ac.il;

Abstract

The study focuses on the model reduction of an internally damped chain of particles confined within a weakening potential well subjected to polyharmonic excitation to investigate the chain's escape dynamics. The chain features strong linear coupling between particles and non-negligible viscous damping forces arising from their relative motion. The potential well is modeled to have no energy dissipation, which means that damping arises solely from the internal interactions among particles and not from their motion through a resisting medium. Polyharmonic excitation frequencies are chosen to excite both the center of mass of the chain and at least one of the internal resonant frequencies, which are significantly higher than the linearized eigenfrequency of the center of mass within the well.

The relative motion of the particles quickly reaches a steady state because of the non-small internal damping, allowing for the derivation of an efficient force field for the center of mass. Eliminating fast dynamics

reduces the system's degrees of freedom to one, employing a probabilistic approach based on the relative motion's probability density function. The reduced 1 DoF model is appropriate to further investigate with various methods established in the literature (e.g., transformation to action-angle coordinates and subsequent averaging; multiple scales).

Keywords: escape, potential well, particle chain, polyharmonic excitation, model reduction, averaging, classical probability density

1 Introduction

Escape from a potential well is an extensively researched topic in the field of nonlinear dynamic systems [1–5], finding applications in various domains including chemical reactions [6, 7], physics of Josephson junctions [8], MEMS devices [9–14], celestial mechanics, and gravitational collapse. It also plays a crucial role in energy harvesting [15] and is closely related to the dynamics of oscillatory systems [16, 17], as well as specific phenomena such as ship capsizing [4, 18]. Despite the significant body of previous research, unresolved issues still require further investigation [19].

Various aspects of the escape phenomenon have been studied. For example, the problem of the sharp minimum of the critical excitation amplitude near the primary resonance has been examined under unlimited potential and homogeneous initial conditions [20]. Another area of research focuses on determining safe basins, which represent non-escaping initial conditions under specific excitations, and investigating integrity measures that quantify the size of the non-escaping set [2, 21–23]. However, providing accurate analytic results for nonquadratic potential wells is challenging. Approximation methods such as Melnikov's method [2] or the use of adiabatic invariants and action-angle variables [24] offer formulas suitable for small excitation values but lose accuracy away from the 1:1 resonance.

Previous studies have addressed the escape problem of weakly damped particles from truncated quadratic potential wells under harmonic excitation, focusing on the location and size of safe escape basins in the initial conditions plane [25]. The escape problem of two strongly coupled particles in a truncated quadratic potential under biharmonic excitation has also been investigated [26]. When the relative vibrations of the particles are significantly faster than the oscillation of the particle's center of mass within the potential, the system can be effectively reduced to a one-degree-of-freedom system by introducing an effective potential. The effective force field is derived by cross-correlating the original potential with the probability density function of the fast relative motion [27]. This study expands the scope of previous investigations by focusing on a strongly coupled n-particle chain subjected to polyharmonic

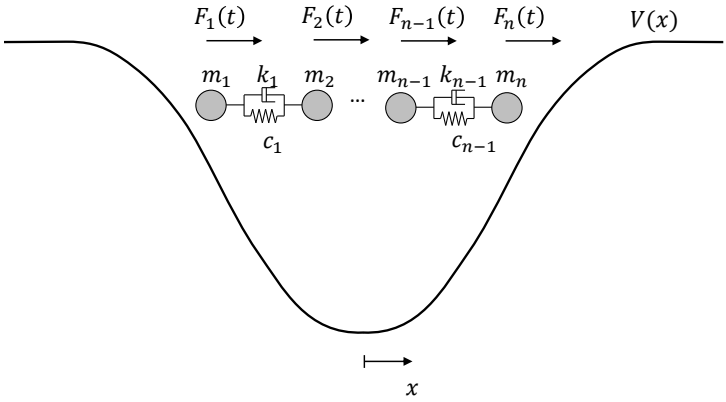

Fig. 1: Problem setting of an internally damped, coupled n-particle system in a potential well, where particles have an equilibrium distance of zero, implying the possibility for mutual penetration without physical constraints

excitation. Additionally, we provide a more rigorous analytical foundation for the method previously employed on a heuristic basis.

The structure of this paper is as follows. Sect. 2 discusses the problem setting and provides the solution for relative vibrations in a chain of n particles. Sect. 3 delves into the model reduction approach based on averaging. Sect. 4 illustrates these concepts with an example involving a three-particle chain. Sect. 5 contains a comprehensive discussion, and, finally, Sect. 6 offers conclusions and highlights the scope for future research.

2 Problem setting

We consider the following problem setting depicted in Fig. 1. The movement is one-dimensional and occurs along the x axis. The masses of the n individual particles are denoted by m_1, m_2, ... , m_n. The damping coefficient of the $n-1$ dashpot dampers is represented by k_1, k_2, ... , k_{n-1}, while the stiffness of the $n-1$ linear springs between the particles is denoted by c_1, c_2, ... , c_{n-1}. Each particle can be stimulated by a polyharmonic force, which is expressed as $F_1(t)$, $F_2(t)$, ... , $F_n(t)$. Initially, the particles are situated in a potential well. For each particle, this is individually given by $V_1(x)$, $V_2(x)$, ... , $V_n(x)$, where $V_i(x) = m_i V(x)$, with $V(x)$ defined in more detail below.

Additionally, it is essential to note that, in this system, the particles can penetrate each other, reflecting that the equilibrium distance between the particles is zero.

2.1 Equations of motion

Applying the Euler-Lagrange equations, we can derive the equations of motion of the above system.

$$\frac{\mathrm{d}}{\mathrm{d}t}\frac{\partial T}{\partial \dot{q}_i}(t,\dot{\mathbf{q}}(t)) = -\frac{\partial U}{\partial q_i}(t,\mathbf{q}(t)) - \frac{\partial D}{\partial \dot{q}_i}(t,\dot{\mathbf{q}}(t)) + Q_i^*(t) \qquad \text{for } i = 1,...,n, \quad (1)$$

where the general coordinates are chosen to be $q_i = x_i$ and

$$T = \sum_{i=1}^{n} \frac{1}{2} m_i \dot{x}_i^2, \quad (2)$$

$$U = \sum_{i=1}^{n-1} \frac{1}{2} c_i (x_{i+1} - x_i)^2 + V_i(x_i), \quad (3)$$

$$D = \sum_{i=1}^{n-1} \frac{1}{2} k_i (\dot{x}_{i+1} - \dot{x}_i)^2, \quad (4)$$

$$Q_i^*(t) = F_i(t) = F_{i,0}\sin(\Omega_0 t + \beta_{i,0}) + \sum_{p=1}^{P} F_{i,p}\sin(\Omega_{i,p} t + \beta_{i,p}), \quad (5)$$

where $P \in \mathbb{N}^+$. We require that the general potential $V(x)$ is bounded above, i.e., it fulfills

$$\lim_{|x|\to\infty} V(x) \leq C, \text{ for some } C \in \mathbb{R}. \quad (6)$$

Furthermore, we require that the potential well has a stable equilibrium at $x = 0$, and its linearized eigenfrequency around this equilibrium is 1, i.e.:

$$V'(x=0) = 0, \quad (7)$$

$$V''(x=0) = 1. \quad (8)$$

Additionally, we assume that $V(x)$ is softening and has a single well, i.e.

$$V''(x) \leq \frac{V'(x)}{x} \leq 1. \quad (9)$$

Ineq. (9) is obtained from the definition of a "softening characteristic," that is, the stiffness of the potential $c(x) := V'(x)/x$ decreases monotonically as the distance from the bottom of the well $|x|$ increases. On the other hand, the maximum stiffness at $x = 0$ is given by

$$\lim_{x\to 0}\frac{V'(x)}{x} = \lim_{x\to 0}\frac{V'(x) - V'(0)}{x - 0} = V''(x)|_{x=0} = 1. \quad (10)$$

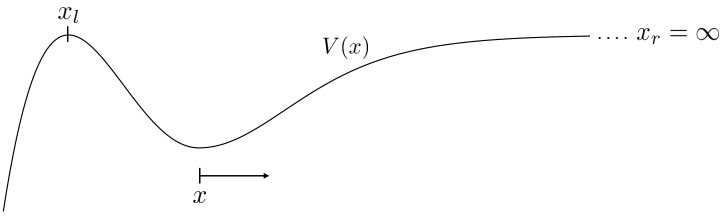

Fig. 2: Example of a feasible potential. The interior of the potential stretches from x_l to x_r

Given that $V(x)$ is bounded above, we define the location of the left supremum of $V(x)$ as x_l, where $x_l \in \mathbb{R}^- \cup \{-\infty\}$, and the location of the right supremum as x_r, where $x_r \in \mathbb{R}^+ \cup \{\infty\}$. We refer to the interval (x_l, x_r) as the *interior* of the well. The term *escape* is used when the chain exits this region. For a detailed definition of escape, see Sect. 2.2.1. Fig. 2 shows a graphical representation of a feasible potential.

We assume that the masses m_i are of magnitude $\mathcal{O}(1)$ and that the forces of the coupling springs are much greater than those of the potential, that is, $c_i \gg 1 \geq \max_{x \in (x_l, x_r)} V_i''(x)$, or equivalently $c_i \in \mathcal{O}(\varepsilon^{-1})$. Additionally, we assume the existence of non-small damping, denoted by $k_i \in \mathcal{O}(1)$. With the above assumptions on c_i and k_i, the chain's internal modes are underdamped (cf. Sect. 2.4). Thus, the corresponding receptance frequency response function has $n-1$ local maxima (cf. Fig. 3). We refer to the location of the local maxima as *resonant frequencies*. We postulate that the lowest resonant frequency of the relative movements in the particle chain significantly exceeds the linearized eigenfrequency of any singular particle in the potential well.

Each particle is excited by up to $P + 1$ harmonic forces. We assume low-frequency excitation for each particle with possibly different amplitudes $F_{i,0}$ and initial phases $\beta_{i,0}$, but with identical frequency $\Omega_0 \in \mathcal{O}(1)$.

The rest of the excitation frequencies are considered significantly higher than the base frequency, i.e., $\Omega_{i,p} \gg \Omega_0$, and are not necessarily identical for all particles, i.e., $\Omega_{i,p}$ is independent of $\Omega_{j,p}$.

Such excitation patterns are relevant in models of cantilever beams used as sensors in Micro-Electro-Mechanical Systems (MEMS). An important application of this can be found in Atomic Force Microscopy (AFM), where a transcendental equation determines the eigenfrequencies of the cantilever beam and are linearly independent over the rational numbers (cf. Def. 2). This example reflects a realistic physical situation where the proposed can be helpful.

Insertion of Eqs. (2-5) in Eq. (1) yields the nonlinear differential equation system

$$\mathbf{M}\ddot{\mathbf{x}} + \mathbf{K}\dot{\mathbf{x}} + \mathbf{C}\mathbf{x} + \mathbf{v}'(\mathbf{x}) = \mathbf{f}(t), \tag{11}$$

where the matrices and vectors are

$$\mathbf{M} = \begin{bmatrix} m_1 & 0 & \dots & & 0 \\ 0 & m_2 & & & \\ & & m_3 & \ddots & \vdots \\ \vdots & & \ddots & \ddots & \\ & & & m_{n-1} & 0 \\ 0 & & \dots & 0 & m_n \end{bmatrix}, \tag{12}$$

$$\mathbf{K} = \begin{bmatrix} k_1 & -k_1 & 0 & \dots & \dots & 0 \\ -k_1 & k_1+k_2 & -k_2 & \ddots & & \vdots \\ 0 & -k_2 & k_2+k_3 & -k_3 & & \vdots \\ \vdots & \ddots & & \ddots & \ddots & 0 \\ \vdots & & \ddots & -k_{n-2} & k_{n-1}+k_{n-2} & -k_{n-1} \\ 0 & \dots & \dots & 0 & -k_{n-1} & k_{n-1} \end{bmatrix}, \tag{13}$$

$$\mathbf{C} = \begin{bmatrix} c_1 & -c_1 & 0 & \dots & \dots & 0 \\ -c_1 & c_1+c_2 & -c_2 & \ddots & & \vdots \\ 0 & -c_2 & c_2+c_3 & -c_3 & & \vdots \\ \vdots & \ddots & & \ddots & \ddots & 0 \\ \vdots & & \ddots & -c_{n-2} & c_{n-1}+c_{n-2} & -c_{n-1} \\ 0 & \dots & \dots & 0 & -c_{n-1} & c_{n-1} \end{bmatrix}, \tag{14}$$

$$\mathbf{x} = \begin{bmatrix} x_1 \\ x_2 \\ x_3 \\ \vdots \\ x_{n-1} \\ x_n \end{bmatrix}, \qquad \mathbf{v}'(\mathbf{x}) = \begin{bmatrix} V_1'(x_1) \\ V_2'(x_2) \\ V_3'(x_3) \\ \vdots \\ V_{n-1}'(x_{n-1}) \\ V_n'(x_n) \end{bmatrix}, \qquad \mathbf{f}(t) = \begin{bmatrix} F_1(t) \\ F_2(t) \\ F_3(t) \\ \vdots \\ F_{n-1}(t) \\ F_n(t) \end{bmatrix}. \tag{15}$$

Furthermore, bold lowercase symbols denote vectors in the time domain, while bold uppercase symbols indicate matrices. Consistent with the standard literature, vectors containing the Laplace transforms of vector values are also represented using bold uppercase letters. The reader is respectfully reminded to be mindful of this notation to avoid any confusion.

2.2 Decoupling coordinate transformation

In the present form, the differential equation is strongly coupled. However, with an appropriate coordinate transform, we can get a system that is only weakly coupled and much easier to handle analytically. We introduce the new coordinates, η and y_i for $i \in \{2, \ldots, n\}$, as follows:

$$\eta = \frac{\sum_{i=1}^{n} m_i x_i}{\sum_{i=1}^{n} m_i}, \tag{16}$$

$$y_i = x_i - x_{i-1}, \qquad \text{for } i \geq 2. \tag{17}$$

Thus, the first coordinate represents the center of mass of the chain, and the rest of the coordinates are the relative distances between two consecutive particles. By defining $M = \sum_{i=1}^{n} m_i$ we can write the transformation as

$$\mathbf{y} = \begin{bmatrix} \eta \\ y_2 \\ y_3 \\ \vdots \\ y_n \end{bmatrix} = \underbrace{\begin{bmatrix} \frac{m_1}{M} & \frac{m_2}{M} & \frac{m_3}{M} & \cdots & \frac{m_n}{M} \\ -1 & 1 & 0 & \ldots & 0 \\ 0 & -1 & 1 & \ddots & \vdots \\ \vdots & \ddots & \ddots & \ddots & 0 \\ 0 & \ldots & 0 & -1 & 1 \end{bmatrix}}_{=:\mathbf{S}^{-1}} \begin{bmatrix} x_1 \\ x_2 \\ x_3 \\ \vdots \\ x_n \end{bmatrix}. \tag{18}$$

Introducing the notation $M_{kl} = \sum_{i=k}^{l} m_i$, with $l > k \in \mathbb{N}^+$, finally we can derive an expression for the matrix $\mathbf{S}$:

$$\mathbf{S} = \frac{1}{M} \begin{bmatrix} M & -M_{2n} & -M_{3n} & \ldots & \ldots & \ldots & -M_{nn} \\ M & M_{11} & -M_{3n} & \ldots & \ldots & \ldots & -M_{nn} \\ M & M_{11} & M_{12} & -M_{4n} & \ldots & \ldots & -M_{nn} \\ \vdots & & & & \ddots & & \vdots \\ M & M_{11} & \ldots & M_{1(k-1)} & -M_{(k+1)n} & \ldots & -M_{nn} \\ M & M_{11} & \ldots & \ldots & \ldots & M_{1(n-2)} & M_{1(n-1)} \end{bmatrix}. \tag{19}$$

Inserting $\mathbf{x} = \mathbf{S}\mathbf{y}$ into Eq. (11), we can write the equations of motion in the new coordinates as

$$\mathbf{M}\mathbf{S}\ddot{\mathbf{y}} + \mathbf{K}\mathbf{S}\dot{\mathbf{y}} + \mathbf{C}\mathbf{S}\mathbf{y} + \mathbf{v}'(\mathbf{S}\mathbf{y}) = \mathbf{f}(t), \tag{20}$$

$$\ddot{\mathbf{y}} + \underbrace{\mathbf{S}^{-1}\mathbf{M}^{-1}\mathbf{K}\mathbf{S}}_{=:\tilde{\mathbf{K}}}\dot{\mathbf{y}} + \underbrace{\mathbf{S}^{-1}\mathbf{M}^{-1}\mathbf{C}\mathbf{S}}_{=:\tilde{\mathbf{C}}}\mathbf{y} + \mathbf{S}^{-1}\mathbf{M}^{-1}\mathbf{v}'(\mathbf{S}\mathbf{y}) = \underbrace{\mathbf{S}^{-1}\mathbf{M}^{-1}\mathbf{f}(t)}_{=:\tilde{\mathbf{f}}(t)}. \tag{21}$$

After some calculations, we obtain the following.

$$\tilde{\mathbf{K}} = \mathbf{S}^{-1}\mathbf{M}^{-1}\mathbf{K}\mathbf{S} = \begin{bmatrix} 0 & 0 & 0 & \dots & \dots & 0 \\ 0 & \frac{k_1}{m_1} + \frac{k_1}{m_2} & -\frac{k_2}{m_2} & 0 & \dots & 0 \\ \vdots & -\frac{k_1}{m_2} & \frac{k_2}{m_2} + \frac{k_2}{m_3} & -\frac{k_3}{m_3} & \ddots & \vdots \\ & \ddots & & \ddots & & 0 \\ \vdots & & 0 & -\frac{k_{n-3}}{m_{n-2}} & \frac{k_{n-2}}{m_{n-2}} + \frac{k_{n-2}}{m_{n-1}} & -\frac{k_{n-1}}{m_{n-1}} \\ 0 & \dots & & 0 & -\frac{k_{n-2}}{m_{n-1}} & \frac{k_{n-1}}{m_{n-1}} + \frac{k_{n-1}}{m_n} \end{bmatrix}. \tag{22}$$

It is clear that in the new coordinates, the inner viscous damping has no more effect on the center of mass η. In the same manner, the calculation of the matrix $\mathbf{S}^{-1}\mathbf{M}^{-1}\mathbf{C}\mathbf{S}$ can be performed resulting in

$$\tilde{\mathbf{C}} = \mathbf{S}^{-1}\mathbf{M}^{-1}\mathbf{C}\mathbf{S} = \begin{bmatrix} 0 & 0 & 0 & \dots & \dots & 0 \\ 0 & \frac{c_1}{m_1} + \frac{c_1}{m_2} & -\frac{c_2}{m_2} & 0 & \dots & 0 \\ \vdots & -\frac{c_1}{m_2} & \frac{c_2}{m_2} + \frac{c_2}{m_3} & -\frac{c_3}{m_3} & \ddots & \vdots \\ & \ddots & & \ddots & & 0 \\ \vdots & & 0 & -\frac{c_{n-3}}{m_{n-2}} & \frac{c_{n-2}}{m_{n-2}} + \frac{c_{n-2}}{m_{n-1}} & -\frac{c_{n-1}}{m_{n-1}} \\ 0 & \dots & 0 & 0 & -\frac{c_{n-2}}{m_{n-1}} & \frac{c_{n-1}}{m_{n-1}} + \frac{c_{n-1}}{m_n} \end{bmatrix}. \tag{23}$$

Further, we calculate

$$\mathbf{S}^{-1}\mathbf{M}^{-1}\mathbf{v}'(\mathbf{S}\mathbf{y}) = \mathbf{S}^{-1}\mathbf{M}^{-1}\begin{bmatrix} m_1 V'(\mathbf{s}_1\mathbf{y}) \\ m_2 V'(\mathbf{s}_2\mathbf{y}) \\ m_3 V'(\mathbf{s}_3\mathbf{y}) \\ \vdots \\ m_n V'(\mathbf{s}_n\mathbf{y}) \end{bmatrix} = \begin{bmatrix} \frac{\sum_{i=1}^{n} m_i V'(\mathbf{s}_i\mathbf{y})}{M} \\ V'(\mathbf{s}_2\mathbf{y}) - V'(\mathbf{s}_1\mathbf{y}) \\ V'(\mathbf{s}_3\mathbf{y}) - V'(\mathbf{s}_2\mathbf{y}) \\ \vdots \\ V'(\mathbf{s}_n\mathbf{y}) - V'(\mathbf{s}_{n-1}\mathbf{y}) \end{bmatrix}, \tag{24}$$

using the notation $\mathbf{S} = (\mathbf{s}_1, \mathbf{s}_1, \dots, \mathbf{s}_n)^{\mathrm{T}}$ with $\mathbf{s}_i \in \mathbb{R}^n$.

Based on [28] and [29], the particular solutions of $y_2 ... y_n$ are only negligibly influenced by their coupling to η, which is due to the strong damping between the particles and the fact that the coupling to the "outer" potential field is weak since $c_i/m_i \in \mathcal{O}(\varepsilon^{-1})$, while maximal stiffness of the potential $\max_{x\in(x_l,x_r)} V'(x)/x$ is of magnitude $\mathcal{O}(1)$.

Considering small relative displacements, i.e., $|y_i| < 1$ for $i = 2...n$, and assuming that the particles are primarily inside of the potential well, i.e.,

$x_i \in (x_l, x_r)$, the force of the potential can be linearized around x_{i-1} as

$$V'(x) \approx V'(x_{i-1}) + V''(x_{i-1})(x - x_{i-1}), \tag{25}$$

and by $\mathbf{s}_i\mathbf{y}_i = x_i$ we find

$$\begin{aligned} V'(\mathbf{s}_i\mathbf{y}) - V'(\mathbf{s}_{i-1}\mathbf{y}) &\approx V'(x_{i-1}) + V''(x_{i-1})(x_i - x_{i-1}) - V'(x_{i-1}) && (26)\\ &= V''(x_{i-1})y_i, && (27)\end{aligned}$$

which we can neglect since $V''(x) \leq 1 \ll c_i$ by our assumptions. Thus, the vector can be rewritten as

$$\mathbf{S}^{-1}\mathbf{M}^{-1}\mathbf{v}'(\mathbf{S}\mathbf{y}) \approx \begin{bmatrix} \frac{\sum_{i=1}^{n} m_i V'(\mathbf{s}_i\mathbf{y})}{M} \\ 0 \\ 0 \\ \vdots \\ 0 \end{bmatrix}. \tag{28}$$

Similarly, we obtain

$$\tilde{\mathbf{f}}(t) = \mathbf{S}^{-1}\mathbf{M}^{-1}\mathbf{f}(t) = \begin{bmatrix} \frac{\sum_{i=1}^{n} F_i(t)}{M} \\ \frac{F_2(t)}{m_2} - \frac{F_1(t)}{m_1} \\ \frac{F_3(t)}{m_3} - \frac{F_2(t)}{m_2} \\ \vdots \\ \frac{F_n(t)}{m_n} - \frac{F_{n-1}(t)}{m_{n-1}} \end{bmatrix}. \tag{29}$$

2.2.1 Escape definition

The definition of escape is, in general, problem-specific, depending on $V(x)$. The following one is suitable for a particle chain in a *single-welled* potential (i.e., the potential has only one local minimum). The chain escapes if "$\exists i \in \{1, \ldots, n\}$ such that $\lim_{t\to\infty}|y_i(t)| = \infty$". This definition allows for the escape of the whole chain in one direction $\lim_{t\to\infty}|\eta(t)| = \infty$, or for the splitting of the chain for $i \in \{2, \ldots, n\}$. Due to the strong coupling between the particles, this second scenario is possible for certain potentials, but only with unrealistically large excitation values; therefore, we do not consider it in the following.

The definition of escape can differ for particles or particle chains in a *multi-welled* potential since the previous definition must not or cannot hold. For example, in the case of a ship capsize, the dynamics is described in angle coordinates, and escape means going from the upright well into a lateral well, but not into infinity.

2.3 The steady-state solutions of $y_2(t)...y_n(t)$

In general, an analytic expression for the eigenmodes and eigenfrequencies, and so, for the particular solutions of $y_2(t)...y_n(t)$, cannot be given with a closed formula. Thus, we limit the investigation to a special case where the masses, the dampers, and the strings are all equal, that is, $m_i = m$ for all $i \in 1, \ldots, n$ and $k_i = k$ and $c_i = c$ for all $i \in 1, \ldots, n-1$. The equation of motion of the center of mass becomes

$$\ddot{\eta} + \frac{\sum_{i=1}^{n} V'(\mathbf{s}_i \mathbf{y})}{n} = \frac{\sum_{i=1}^{n} F_i(t)}{nm}. \tag{30}$$

To address Eq. (30), it is essential first to obtain solutions for $y_2, \ldots, y_n$, which necessitates focusing on the submatrix formed by excluding the first row and column of our current matrices, which leads to the following simplified expressions.

$$\bar{\mathbf{y}} = [y_2 \quad y_3 \quad \ldots \quad y_n]^\top \in \mathbb{R}^{n-1}, \tag{31}$$

$$\bar{\mathbf{K}} = \tilde{\mathbf{K}}_{2:n,2:n} \in \mathbb{R}^{(n-1)\times(n-1)}, \tag{32}$$

$$\bar{\mathbf{C}} = \tilde{\mathbf{C}}_{2:n,2:n} \in \mathbb{R}^{(n-1)\times(n-1)}, \tag{33}$$

$$\bar{\mathbf{f}} = \tilde{\mathbf{f}}_{2:n} \in \mathbb{R}^{n-1}, \tag{34}$$

where $p : q$ in the vector index denotes the vector obtained by taking the entries from the p^{th} row to the q^{th} row. Similarly, $p : q, r : s$ in the matrix index denotes the matrix block obtained by taking the entries between the rows p and q and between the columns r and s. The equations of motion of the reduced system can be written as

$$\ddot{\bar{\mathbf{y}}} + \bar{\mathbf{K}}\dot{\bar{\mathbf{y}}} + \bar{\mathbf{C}}\bar{\mathbf{y}} = \bar{\mathbf{f}}(t), \tag{35}$$

where $\bar{\mathbf{K}}$ and $\bar{\mathbf{C}}$ are tridiagonal Toeplitz matrices.

As the chosen damping value is non-small, the homogeneous equation will decay rapidly. Hence, we are only interested in the particular solution given to the polyharmonic excitation. Using the linearity of the problem, we can obtain the solution by applying the Laplace transform. Assuming zero initial conditions, the Laplace transform of Eq. (35) becomes

$$s^2\bar{\mathbf{Y}}(s) + s\bar{\mathbf{K}}\bar{\mathbf{Y}}(s) + \bar{\mathbf{C}}\bar{\mathbf{Y}}(s) = \bar{\mathbf{F}}(s), \tag{36}$$

where $\bar{\mathbf{Y}}(s) = \mathcal{L}\{\bar{\mathbf{y}}(t)\}$ and $\bar{\mathbf{F}}(s) = \mathcal{L}\{\bar{\mathbf{f}}(t)\}$, which is equivalent to

$$\underbrace{\begin{bmatrix} s^2+2\frac{k}{m}s+2\frac{c}{m} & -\frac{k}{m}s-\frac{c}{m} & 0 & \dots & 0 \\ -\frac{k}{m}s-\frac{c}{m} & \ddots & \ddots & \ddots & \vdots \\ 0 & \ddots & \ddots & \ddots & 0 \\ \vdots & \ddots & \ddots & \ddots & -\frac{k}{m}s-\frac{c}{m} \\ 0 & \dots & 0 & -\frac{k}{m}s-\frac{c}{m} & s^2+2\frac{k}{m}s+2\frac{c}{m} \end{bmatrix}}_{=:\mathbf{A}(s)} \begin{bmatrix} Y_2 \\ Y_3 \\ \vdots \\ Y_{n-1} \\ Y_n \end{bmatrix} = \begin{bmatrix} \bar{F}_2 \\ \bar{F}_3 \\ \vdots \\ \bar{F}_{n-1} \\ \bar{F}_n \end{bmatrix}. \tag{37}$$

Let us denote the values of the main diagonal with $a = s^2 + 2\frac{k}{m}s + 2\frac{c}{m}$ and with $b = -\frac{k}{m}s - \frac{c}{m}$ the values of the sub and superdiagonals. Based on [30] the eigenvalues λ_k, $k = 1...n-1$ of the matrix are given as

$$\lambda_k = a - 2b\cos\left(\frac{k\pi}{n}\right), \tag{38}$$

and the eigenvectors are

$$\mathbf{v}^k = \left[\sin\left(\frac{\pi k}{n}\right), \dots, \sin\left(\frac{(n-1)\pi k}{n}\right)\right]^\top, \text{ for } k \in \{1, \dots, n-1\}. \tag{39}$$

The eigenvectors do not have a unit length in this representation, so the next step is to normalize them:

$$\left|\mathbf{v}^k\right| = \sqrt{\sin^2\left(\frac{\pi k}{n}\right) + \sin^2\left(\frac{2\pi k}{n}\right) + \dots + \sin^2\left(\frac{(n-1)\pi k}{n}\right)}, \tag{40}$$

and using the trigonometrical identity $\sin^2 x = \frac{1-\cos 2x}{2}$ we obtain

$$\left|\mathbf{v}^k\right| = \sqrt{\frac{1-\cos\left(\frac{2\pi k}{n}\right)}{2} + \frac{1-\cos\left(\frac{4\pi k}{n}\right)}{2} + \dots + \frac{1-\cos\left(\frac{2(n-1)\pi k}{n}\right)}{2}}, \tag{41}$$

$$\left|\mathbf{v}^k\right| = \sqrt{\frac{n-1}{2} - \frac{1}{2}\underbrace{\sum_{l=1}^{n-1}\cos\left(\frac{2\pi lk}{n}\right)}_{=-1}}, \tag{42}$$

$$\left|\mathbf{v}^k\right| = \sqrt{\frac{n}{2}}, \tag{43}$$

where the sum with the cosine term is -1 since the sum consists of all the n roots of unity except the root one. As it is well known, the roots of unity add

up to zero. Therefore, the above sum always adds up to -1. The matrix

$$\mathbf{Q} = \sqrt{\frac{2}{n}} \left[\mathbf{v}^1, \, \mathbf{v}^2, \, \ldots, \, \mathbf{v}^{n-1} \right] \tag{44}$$

is orthogonal and symmetric, i.e., $\mathbf{Q} = \mathbf{Q}^{-1} = \mathbf{Q}^{\top}$. The matrix $\mathbf{A} \in \mathbb{C}^{(n-1)\times(n-1)}$ can be written as

$$\mathbf{A} = \mathbf{Q}\mathbf{\Lambda}\mathbf{Q}^{\top} = \mathbf{Q}\mathbf{\Lambda}\mathbf{Q}, \tag{45}$$

and so due to the above-mentioned properties the inverse of $\mathbf{A}$ can be written as

$$\mathbf{A}^{-1} = \mathbf{Q}\mathbf{\Lambda}^{-1}\mathbf{Q}. \tag{46}$$

We can give the entries of $\mathbf{A}^{-1}$ as follows.

$$A_{ij}^{-1}(s) = \frac{2}{n} \sum_{k=1}^{n-1} \frac{\sin\left(\frac{i\pi k}{n}\right) \sin\left(\frac{j\pi k}{n}\right)}{a + 2b\cos\left(\frac{k\pi}{n}\right)}, \tag{47}$$

where $i, j = 1...n-1$. After substituting the values of a and b, we can write

$$A_{ij}^{-1}(s) = \frac{2}{n} \sum_{l=1}^{n-1} \frac{\sin\left(\frac{i\pi l}{n}\right) \sin\left(\frac{j\pi l}{n}\right)}{s^2 + 2\frac{k}{m}s + 2\frac{c}{m} - 2\left(\frac{k}{m}s + \frac{c}{m}\right)\cos\left(\frac{\pi l}{n}\right)}. \tag{48}$$

The particular solution can be found using the system's linearity for polyharmonic excitation. We can first calculate the effect of a harmonic excitation and then take the superposition of all excitations that act on the particle chain.

To start with, we investigate the response to the harmonic $F_i \sin(\omega_i t + \beta_i)$, acting at the $i^{\text{th}} \in \{1, \ldots, n-1\}$ reduced coordinate, not to be confused with the i^{th} particle. We find

$$\bar{\mathbf{Y}}(s = j\omega_i) = \mathbf{A}^{-1}(j\omega_i) \begin{bmatrix} 0 \\ \vdots \\ F_i e^{j\beta_i} \\ \vdots \\ 0 \end{bmatrix} = F_i e^{j\beta_i} \mathbf{a}_i^{-1}(j\omega_i), \tag{49}$$

where $\mathbf{a}_i^{-1}$ denotes the i^{th} column of the matrix $\mathbf{A}^{-1}$ and j is the imaginary unit. Then the k^{th} row of vector $\bar{\mathbf{y}}(t)$ has the form

$$\bar{y}_k(t) = \left|\bar{Y}_k(\omega_i)\right| \sin(\omega_i t + \bar{\Psi}_k(\omega_i)), \tag{50}$$

where $\bar{\Psi}_k(\omega_i) = \angle \bar{Y}_k(\omega_i)$ is the phase angle.

If we excite the i^{th} particle according to Eq. 5 in the y coordinates, this excitation manifests twice, as indicated by Eq. 29, except at the chain ends where it occurs only once. Consequently, we have $2(P+1)(n-1)$ distinct harmonic terms superimposed.

Let us define $\bar{\mathbf{Y}}_{i,p,+}$ and $\bar{\mathbf{Y}}_{i,p,-}$ as the complex amplitudes of the simple harmonic excitation caused by the p^{th} harmonic excitation, $p \in \{0,\dots,P\}$, of the i^{th} particle, $i \in \{1,2,\dots,n\}$ when having a plus or minus sign as in Eq. (29):

$$\bar{\mathbf{Y}}_{i-1,p,+}(j\Omega_{i,p}) = F_{i,p}e^{j\beta_{i,p}}\mathbf{a}_i^{-1}(j\Omega_{i,p}), \qquad i \in \{2,\dots,n\}, \quad p \in \{0,1,\dots,P\}, \tag{51}$$

$$\bar{\mathbf{Y}}_{i,p,-}(j\Omega_{i,p}) = -F_{i,p}e^{j\beta_{i,p}}\mathbf{a}_i^{-1}(j\Omega_{i,p}), \quad i \in \{1,2,\dots,n-1\}, \quad p \in \{0,1,\dots,P\}. \tag{52}$$

The particular solution of the relative distances become

$$y_k(t) = \sum_{i=1}^{n-1}\sum_{p=0}^{P}\sum_{q\in\{-,+\}} \left|\bar{Y}_{i,p,q,k-1}(j\Omega_{i,p})\right| \sin(\Omega_{i,p}t + \bar{\Psi}_{i,p,q,k-1}(j\Omega_{i,p})), \tag{53}$$

with $k \in \{2,\dots,n\}$, and $\bar{Y}_{i,p,q,k-1}$ denoting the $(k-1)^{\text{th}}$ row of the vector $\bar{\mathbf{Y}}_{i,p,q}$. Thus, we obtain accurate estimates for $y_2(t),\dots,y_n(t)$.

2.4 Resonant frequencies

We are generally interested in the system's behavior near its resonant frequencies. Therefore, we derive the frequencies of the resonance peaks and the relative amplifications at these points. In order to do that, it is enough to examine the system with a single harmonic excitation, as given in Eq. (49), which acts on the i^{th} reduced coordinate (not on the i^{th} particle). Writing the explicit expression for the k^{th} row of the vector, we have

$$\bar{Y}_k(j\omega_i) = \frac{2}{n}\sum_{l=1}^{n-1} \left.\frac{\sin\left(\frac{i\pi l}{n}\right)\sin\left(\frac{k\pi l}{n}\right)}{s^2 + 2\frac{k}{m}s + 2\frac{c}{m} - 2\left(\frac{k}{m}s + \frac{c}{m}\right)\cos\left(\frac{\pi l}{n}\right)}\right|_{s=j\omega_i} F_i e^{\beta_i} \tag{54}$$

$$= \frac{2}{n}\sum_{l=1}^{n-1} \frac{\sin\left(\frac{i\pi l}{n}\right)\sin\left(\frac{j\pi l}{n}\right)}{\left[2\frac{c}{m}\left(1-\cos\left(\frac{\pi l}{n}\right)\right) - \omega_i^2\right] - j\left[2\omega_i\frac{k}{m}\left(1-\cos(\frac{\pi l}{n})\right)\right]} F_j e^{\beta_j}. \tag{55}$$

Large vibrations can occur when $|Y_i|$ is large, that is, when at least one of the denominators in the sum approaches zero in its absolute value. The absolute value of the denominator is

$$\left|\left[\frac{2c}{m}\left(1-\cos\left(\frac{\pi l}{n}\right)\right) - \omega_i^2\right] - j\left[2\omega_i\frac{k}{m}\left(1-\cos\left(\frac{\pi l}{n}\right)\right)\right]\right| = \tag{56}$$

$$\sqrt{\left[\frac{2c}{m}\left(1-\cos\left(\frac{\pi l}{n}\right)\right) - \omega_i^2\right]^2 + 4\omega_i^2\frac{k^2}{m^2}\left(1-\cos\left(\frac{\pi l}{n}\right)\right)^2} = \tag{57}$$

$$\sqrt{\omega_i^4 + 4\left(1-\cos\left(\frac{l\pi}{n}\right)\right)\left[\frac{k^2}{m^2}\left(1-\cos\left(\frac{l\pi}{n}\right)\right)-\frac{c}{m}\right]\omega_i^2+\left(\frac{2c}{m}\left(1-\cos\frac{\pi l}{n}\right)\right)^2}. \tag{58}$$

Since $k > 0$, the absolute value of the denominator is a continuously differentiable function for any $\omega_i \in \mathbb{R}$, and we can find its minimum value by setting its derivative equal to zero.

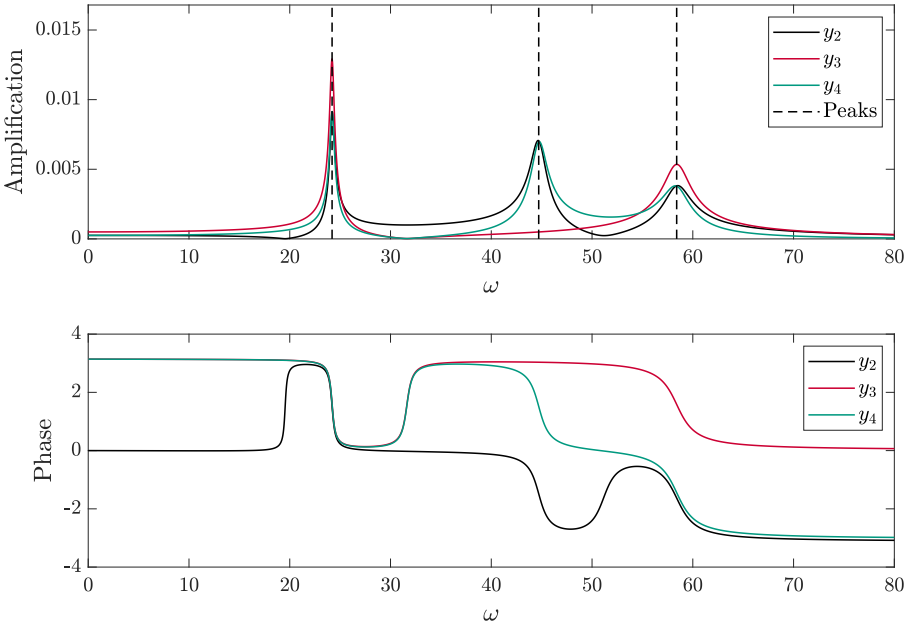

Fig. 3: Amplification and phase depicted against the excitation frequency with $n = 4$ particles for $m = 1$, $k = 0.8$, $c = 1000$. The second particle of the chain is excited. The analytic peak frequencies given by Eq. (60) are depicted with dashed black lines

Moreover, since the square root function is monotonic, the expression attains its minimum value, where the fourth-order polynomial inside the root reaches its minimum. Given that this polynomial is symmetric and ω_i^4 has a positive coefficient, two scenarios can be anticipated. In the first scenario, the polynomial reaches its local maximum at $\omega_i = 0$, and its two local minima occur symmetrically around this point. In the second scenario, there is a single local minimum at $\omega_i = 0$, and as we move away from zero, the function values increase monotonically. The latter case corresponds to a strongly overdamped aperiodic system, which is not within the focus of our study (cf. Eq. (65)). We obtain the following result upon differentiating the expression inside the square root.

$$4\omega_i^3 + 8\left(1-\cos\left(\frac{l\pi}{n}\right)\right)\left(\frac{k^2}{m^2}\left(1-\cos\left(\frac{l\pi}{n}\right)\right)-\frac{c}{m}\right)\omega_i = 0, \tag{59}$$

which is solved by

$$\omega_{i,12} = \pm\sqrt{2\left(1-\cos\left(\frac{l\pi}{n}\right)\right)\left(\frac{c}{m}-\frac{k^2}{m^2}\left(1-\cos\left(\frac{l\pi}{n}\right)\right)\right)}, \tag{60}$$

$$\omega_{i,3} = 0. \tag{61}$$

Substituting values for $l = 1...n-1$, we obtain reasonable analytic estimates for the resonant frequencies of the particle chain. A graphical example with $n = 4$ particles is shown in Fig. 3.

Based on Eq. (60), we can also give an estimate for the maximal value of the damping coefficient k_{crit}, for which all internal modes of the chain are oscillatory. If the expression under the square root for all $l \in \{1,\dots,n-1\}$ is real, all resonant peaks exist. Which is the case for

$$\frac{c}{m} > \frac{k^2}{m^2}\left(1-\cos\left(\frac{l\pi}{n}\right)\right), \quad \forall l \in \{1,\dots,n-1\}, \tag{62}$$

$$cm > k^2\left(1-\cos\left(\frac{(n-1)\pi}{n}\right)\right), \tag{63}$$

$$cm > k^2\left(1+\cos\left(\frac{\pi}{n}\right)\right), \tag{64}$$

$$\sqrt{\frac{cm}{2}} > \sqrt{\frac{cm}{1+\cos\frac{\pi}{n}}} =: k_{\text{crit}} > k. \tag{65}$$

Possible values of n range from 2 to ∞, thus the critical damping coefficient has the range

$$k_{\text{crit}} \in \left(\sqrt{\frac{cm}{2}}, \sqrt{cm}\right]. \tag{66}$$

2.5 Special case: harmonic excitation

In the equations of relative motion, the potential force is of the order $\mathcal{O}(1)$ and considered negligible compared to the forces of linear springs of order $\mathcal{O}(\varepsilon^{-1})$. Consequently, the equations are linearized. Owing to the validity of the superposition principle for this simplified linear system, our primary interest is directed towards the behavior of the i^{th} body when it undergoes simple harmonic excitation.

In order to examine the motion relative to the common center of mass of the particles, it is necessary to find the analytic solutions for $y_2(t),\dots,y_n(t)$ under excitation solely by the high-frequency force $F_{i,p}\sin(\Omega_{i,p}t+\beta_{i,p})$, where $p \in \{1,\dots,P\}$. The equation governing η is an undamped second-order nonlinear differential equation. The absence of damping implies that the motion never settles into a steady state. In contrast, the system of equations that describe

the evolution of $y_2(t), \ldots, y_n(t)$ can be well approximated by a damped linear second-order differential equation system. Due to the significant damping, the motion rapidly converges to the steady-state solution as given by Eq. (53). In the case of single harmonic excitation, steady-state solutions $y_2(t), \ldots, y_n(t)$ are all pure harmonics. The following gives the oscillations around the center of mass $\eta(t)$.

$$\begin{aligned}
\mathbf{z}(t) :&= \mathbf{x}(t) - \eta(t)\mathbf{e} && (67)\\
&= \mathbf{S}\mathbf{y}(t) - \eta(t)\mathbf{e}, && (68)\\
&= \frac{1}{n} \underbrace{\begin{bmatrix} -(n-1) & -(n-2) & \ldots & -1 \\ 1 & -(n-2) & \ldots & -1 \\ 1 & 2 & \ldots & -1 \\ \vdots & \vdots & \ddots & \vdots \\ 1 & 2 & \ldots & n-1 \end{bmatrix}}_{\in \mathbb{R}^{n\times(n-1)}} \begin{bmatrix} y_2 \\ y_3 \\ \vdots \\ y_n \end{bmatrix}, && (69)
\end{aligned}$$

with $\mathbf{e} = [1 \quad 1 \quad \ldots \quad 1]^\top$. Due to Eq. (69), the entries of $\mathbf{z}$ are all linear combinations of $y_2, \ldots, y_n$. The sum consists of $n-1$ sine functions with different amplitudes and phases but with identical frequency $\Omega_{i,p}$. The following trigonometric identity is helpful for such an addition of sine functions.

$$\sum_{i=1}^{n} A_i \sin(\omega t + \varphi_i) = A \sin(\omega t + \varphi), \tag{70}$$

with

$$A = \sqrt{\left(\sum_{i=1}^{n} A_i \cos\varphi_i\right)^2 + \left(\sum_{i=1}^{n} A_i \sin\varphi_i\right)^2}, \tag{71}$$

$$\varphi = \operatorname{atan2}\left(\sum_{i=1}^{n} A_i \sin\varphi_i, \sum_{i=1}^{n} A_i \cos\varphi_i\right), \tag{72}$$

where $\operatorname{atan2}(y, x)$ denotes the two-argument arctangent, a more precise version of $\arctan(y/x)$, by providing phase information on $(-\pi, \pi)$, rather than only on $(-\pi/2, \pi/2)$. To determine the amplitude and phase of the harmonic oscillation of the j^{th} body, the use of complex numbers is advantageous, using the solution obtained in Eq. (49) for $\bar{\mathbf{Y}}(j\Omega_{j2})$:

$$\begin{aligned}
\mathbf{Z}(j\Omega_{j2}) &= \bar{\mathbf{S}}\bar{\mathbf{Y}}(j\Omega_{j2}), && (73)\\
A_k &= |Z_k(j\Omega_{j2})|, && (74)\\
\Psi_k &= \angle Z_k(j\Omega_{j2}), && (75)
\end{aligned}$$

$$z_k(t) = A_k \sin(\Omega_{j2} t + \Psi_k). \tag{76}$$

These equations indicate that the relative motions of the particles around the center of mass are expressible as sinusoidal functions. Although these functions share the same frequency, their amplitude and phase values differ.

When subjected to multiple harmonics simultaneously, the linearity of Eq. (35) allows the development of complex relative motions $\mathbf{z}(t)$ within the particle chain around its center of mass. These motions result from the superposition of sinusoidal functions of varying frequencies. The number of frequencies in the excitation force directly equates to the number of sinusoidal functions involved.

Furthermore, given our strong coupling assumption between the particles, it becomes clear that the frequencies that excite the center of mass of the particle chain within the potential well are significantly lower than those that provoke internal vibrations. Consequently, we can effectively neglect the low-frequency excitation terms in calculating $\mathbf{z}$. For a graphical illustration, refer to Fig. 5 in Sect. 4.

Considering this, we can now revisit Eq. (30). To simplify the equation, we will employ a method proposed by *Genda et al.* [26], which models the high-frequency oscillations based on the classical probability density of the position of the particles. This approach offers a straightforward means of capturing the system's dynamics.

3 Averaging-based model reduction

In the previous section, we have derived analytic expressions for the motion of particles around their common center of mass. These can be substituted into Eq. (30). Making use of Eq. (69), we obtain

$$\ddot{\eta} + \frac{\sum_{i=1}^{n} V'(\eta + z_i(t))}{n} = \frac{\sum_{i=1}^{n} F_i(t)}{nm}. \tag{77}$$

Considering that $z_i(t)$ and $F_{i,p} \sin(\Omega_{i,p} t + \beta_{i,p})$ are "fast," we can average the equation and keep only the "slow" dynamics of the system. To denote the averaged position of the center of mass, we introduce $\xi := \langle \eta \rangle$. The fast harmonic forces all vanish, and we obtain the following result.

$$\ddot{\xi} + \left\langle \frac{\sum_{i=1}^{n} V'(\xi + z_i(t))}{n} \right\rangle = \frac{\sum_{i=1}^{n} F_{i,0} \sin(\Omega_0 t + \beta_{i,0})}{nm}. \tag{78}$$

Using Eq. (70) we can reduce Eq. (78) further as

$$\ddot{\xi} + \left\langle \frac{\sum_{i=1}^{n} V'(\xi + z_i(t))}{n} \right\rangle = F_0 \sin(\Omega_0 t + \beta_0), \tag{79}$$

with

$$F_0 := \frac{\sqrt{\left(\sum_{i=1}^{n} F_{i,0}\cos\beta_{i,0}\right)^2 + \left(\sum_{i=1}^{n} F_{i,0}\sin\beta_{i,0}\right)^2}}{nm}, \tag{80}$$

$$\beta_0 := \operatorname{atan2}\left(\sum_{i=1}^{n} F_{i,0}\sin\beta_{i,0}, \sum_{i=1}^{n} F_{i,0}\cos\beta_{i,0}\right), \tag{81}$$

The averaging of the left-hand side of Eq. (78) takes more effort. [27] showed that the time average of the function $f(x + g(t))$, where $g(t)$ represents the "fast" variable, can be obtained not only by a time integral but also by a cross-correlation integral of $f(x)$ and the classical probability density (CPD) $\rho(x)$ of $g(t)$, that is,

$$\langle f(x + g(t))\rangle = \frac{1}{T}\int_0^T f(x + g(t))\mathrm{d}t = \int_{-\infty}^{\infty} f(y)\rho(y - x)\mathrm{d}y. \tag{82}$$

Additionally, [27] demonstrated that the averaged function can be expressed using the moments of the classical probability density $\rho(x)$ for analytic functions. The expression is given by:

$$\langle f(x + g(t))\rangle = \int_{-\infty}^{\infty} f(y)\rho(y - x)\mathrm{d}y = \sum_{k=0}^{\infty} m_k \frac{f^{(k)}(x)}{k!}. \tag{83}$$

Here, m_k represents the k^{th} moment of $\rho(x)$. The result is valid if the support of $\rho(x)$ lies within the convergence domain of the Taylor series expansion of $f(x)$.

Hence, once the moments of the "fast" variables $z_i(t)$ are known, the averaging of Eq. (79) is straightforward, which is especially true if $f(x)$ is some polynomial of order p, in which case only the first p moments must be calculated.

3.1 Derivation of the CPD and moments of the fast motion

The CPDs of various functions have been derived in the literature [27, 31].

The 0^{th} moment for any CPD is invariably 1. In our specific case, $z_i(t)$ approximates a polyharmonic function, which is the superposition of multiple harmonic components. Given certain conditions, moments of this polyharmonic sum can also be ascertained. It is well-established that the probability density function (PDF) for a sum of independent variables can be derived through the convolution of their individual PDFs [32]. CPDs exhibit identical mathematical characteristics to PDFs; they are nonnegative and integrate to 1. However, the variables they represent differ fundamentally. Unlike random

variables, which their PDFs fully characterize, CPDs are formed by disregarding the precise timing of particle positions. They retain information on spatial distribution by accounting solely for the duration for which a particle resides at a specific location. Theorem 1 offers an analytical method for determining the CPD of polyharmonic functions.

Definition 1 (Classical probability density) The *classical probability density* of a particle $\rho(x)$ describes the probability with which a particle in a given observation interval starting at t_0 and ending at t_1 spends an infinitesimal amount of time $\mathrm{d}t$ in the $\mathrm{d}x$ vicinity of a given value x, that is,

$$\rho(x)\mathrm{d}x \propto \mathrm{d}t. \tag{84}$$

Note that since $\rho(x)$ is a probability density function, it must be nonnegative and have a total area of 1. Therefore, the proportionality factor is the inverse of the time interval length $T = t_1 - t_0$, resulting in

$$\rho(x)\mathrm{d}x = \frac{1}{T}\mathrm{d}t. \tag{85}$$

Now, we multiply both sides of Eq. (85) by $1 = \mathrm{d}x/\mathrm{d}x$, we find

$$\rho(x)\mathrm{d}x = \frac{1}{T}\frac{\mathrm{d}x}{\mathrm{d}x/\mathrm{d}t} = \frac{1}{T}\frac{\mathrm{d}x}{v(x)}, \tag{86}$$

where $v(x)$ is the velocity of the particle, resulting in

$$\rho(x) = \frac{1}{T}\frac{1}{v(x)}. \tag{87}$$

In addition, note that the CPD of a particle following the path $x = g(t)$, with a strictly monotonically increasing, continuously differentiable $g(t)$, can be written as

$$\rho(x) = \frac{1}{T}\frac{1}{g'(g^{-1}(x))}. \tag{88}$$

For further explanation, see [27].

Definition 2 (Linear independence over $\mathbb{Q}$) The numbers $\omega_1, \ldots, \omega_P \in \mathbb{R}$ are said to be linearly independent over $\mathbb{Q}$ if

$$\sum_{i=1}^{P} r_i\omega_i \neq 0, \tag{89}$$

for any $r_i \in \mathbb{Q}$, except $r_1 = ... = r_P = 0$.

Weyl showed that the P-dimensional flow on a torus $\mathbb{T}^P = \mathbb{R}^P/\mathbb{Z}^P$ is equidistributed [33], i.e., a particle starting at $\boldsymbol{x_0} = [x_{0,1}, \ldots, x_{0,P}]^\top \in \mathbb{T}^P$ and moving with uniform velocity in the direction $\boldsymbol{\omega} = [\omega_1, \ldots, \omega_P]^\top \in \mathbb{R}^P$ on $\mathbb{T}^P$, i.e.,

$$\mathbf{x}(t) = (\mathbf{x}_0 + \boldsymbol{\omega} t) \bmod 1 = \begin{pmatrix} \{x_{0,1} + \omega_1 t\} \\ \{x_{0,2} + \omega_2 t\} \\ \vdots \\ \{x_{0,P} + \omega_P t\} \end{pmatrix}, \tag{90}$$

has a relative dwell time in any volume element V as indicated by the hypervolume of the volume element $|V|$, if and only if the numbers $\omega_1, \ldots, \omega_P$ are linearly independent over $\mathbb{Q}$.

Here, $\{\cdot\}$ signifies the fractional part function. By *relative dwell time*, we refer to the limit $\lim_{t\to\infty} \frac{t_V}{t}$, where t_V represents the time spent within the volume element V over the entire observation period t. This concept is congruent with the idea that flow on a P-dimensional torus is ergodic with respect to the Haar measure on $\mathbb{T}^P$ [34].

Consequently, if we sample particle positions in uniformly distributed random time instances within the interval $[0, T]$, as $T \to \infty$, the positions sampled during these instances will adhere to a uniform multivariate distribution in $\mathbb{T}^P$. We can interpret these positions as the realizations of a P-dimensional random variable $\mathbf{X} = [X_1, \ldots, X_P]^\top$, where the scalar components are uniformly distributed in $[0, 1]$ and are mutually independent. This understanding enables us to compute the CPD for a polyharmonic excitation as described.

Theorem 1 *Assume that the frequencies $\omega_1, \ldots, \omega_P$ are linearly independent over $\mathbb{Q}$. Then, the CPD of*

$$z(t) = \sum_{i=1}^{P} A_i \sin(\omega_i t + \beta_i) \tag{91}$$

can be obtained by

$$\rho(x) = (\rho_1 * \rho_2 * \ldots * \rho_P)(x), \tag{92}$$

where $\rho_1 * \rho_2 * \ldots * \rho_P$ denotes the convolution of the functions $\rho_1, \rho_2, \ldots, \rho_P$, which are given by the arcsine distribution

$$\rho_i(x) = \frac{1}{\pi\sqrt{A_i^2 - x^2}}. \tag{93}$$

Proof As previously demonstrated, the line on $\mathbb{T}^P$ parameterized by the arguments of the sines is ergodic, which is synonymous with the flow of these arguments on $\mathbb{T}^P$ being uniform. In other words, sampling coordinates of this flow at uniformly randomly selected times produces statistics equivalent to those of a P-dimensional

uniform distribution on the torus, which suggests that the sum in Eq. (91) yields the same probability distribution as the sum of P uniformly distributed, random variables on $[0, 2\pi]$, after applying the transformation $A_i \sin(\Omega_i X_i + \beta_i)$, respectively.

Using Eq. (88), the CPD of a simple harmonic term $A_i \sin(\Omega_i t + \beta_i)$ is readily given by Eq. (93). CPDs and PDFs share the same statistical properties.

Furthermore, it is well known [35] that the PDF of the sum of independent random variables is given by the convolution of the individual PDFs (cf. Eq. (92)), which finishes the proof of the theorem. □

Remark 1 Since the convolution is commutative, it does not matter in which order the operations are performed.

Remark 2 The moments of the centered arcsine distribution with half-width A are given by [27]

$$m_k = \begin{cases} A^k \frac{1}{2^k} \binom{k}{k/2} & \text{for } k \text{ even}, \\ 0 & \text{for } k \text{ odd}, \end{cases} \quad \text{for } k \geq 0. \tag{94}$$

Theorem 2 *Let m_{j,j_i} be the j_i^{th} moment of the j^{th} term's CPD in Eq. (91) with $j_i \in \mathbb{N}^+$ for all $j = \{1, \ldots, P\}$. The k^{th} moment of $\rho(x)$ in Eq. (92) is given by*

$$m_k = \left(\sum_{(\sum_{j=1}^{P} j_i)=k} \prod_{j=1}^{P} \frac{m_{j,j_i}}{j_i!} \right) k! \tag{95}$$

Proof The moment-generating function of a random variable X has the form

$$M_X(t) = \sum_{k=0}^{\infty} \frac{m_k}{k!} t^k. \tag{96}$$

It is well-known that the product of the moment-generating functions of independent random variables $X_1, X_2, \ldots, X_P$ yields the moment-generating function of the random variable that is obtained by the sum of $X_1, X_2, \ldots, X_P$ [36]. In other words, the moment-generating function of $X = \sum_{i=1}^{P} X_i$ is given by

$$M_X(t) = M_{X_1}(t) M_{X_2}(t) ... M_{X_P}(t). \tag{97}$$

Since the moment-generating functions are power series, the Cauchy product rule can be applied, resulting in Eq. (95). □

By combining Eq. (83) with Theorem 2, the effective restoring force in Eq. (79) can be obtained. Still, in general, solving Eq. (83) may still be difficult or only numerically possible. However, if $V(x)$ is a polynomial potential, the results are straightforward and can be obtained analytically.

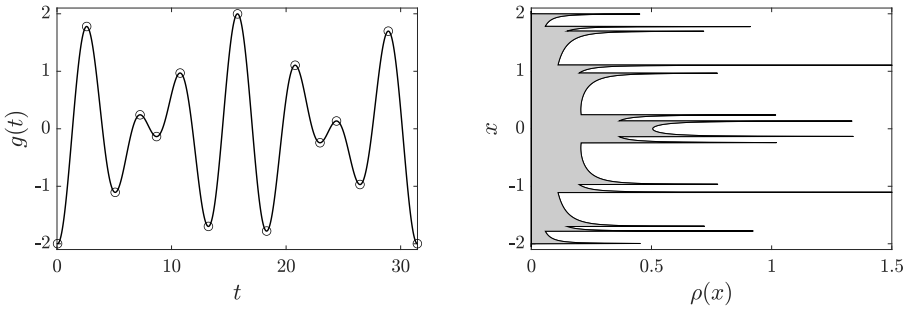

(a) Periodic, bi-harmonic motion given by $g(t) = -\cos(t) - \cos(1.4t - 0.1)$ and its numerically obtained CPD

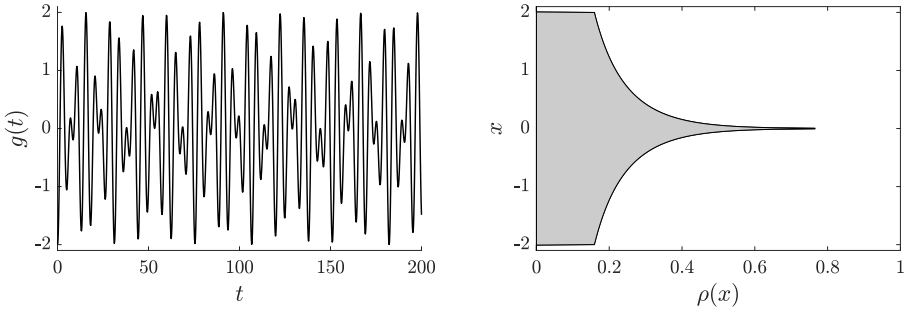

(b) Aperiodic, bi-harmonic motion given by $g(t) = -\cos(t) - \cos(\sqrt{2}t - 0.1)$ and its analytically obtained CPD (see Eq. (127))

Fig. 4: Comparison of commensurability effects on the CPD of motion. Figures reused from [27]

Thus, the reduction of the originally n degree-of-freedom system to a 1 DoF system is complete, given that the distinct "fast" excitation frequencies $\Omega_{i,p}$ are linearly independent over $\mathbb{Q}$. A graphical example showing the differences in the CPDs for commensurable and incommensurable ω_1 and ω_2 is shown in Fig. 4.

In what follows, we present examples illustrating the utility of the analytic results discussed earlier. After reducing the system to 1 DoF, there are numerous methods documented in the existing literature for further analyzing the escape behavior of the system [20, 26, 37–39]. Thus, the focus will be primarily on the reduction process rather than on subsequent analytic approaches specific to 1 DoF escape issues.

4 Example

In the following, we consider an example with $n = 3$ and

$$V(x) = \frac{x^2}{2} - \frac{x^4}{4}. \tag{98}$$

Without loss of generality, we consider $m = 1$. The equations of motion are given by

$$\begin{bmatrix} \ddot{x}_1 \\ \ddot{x}_2 \\ \ddot{x}_3 \end{bmatrix} + \begin{bmatrix} k & -k & 0 \\ -k & 2k & -k \\ 0 & -k & k \end{bmatrix} \begin{bmatrix} \dot{x}_1 \\ \dot{x}_2 \\ \dot{x}_3 \end{bmatrix} + \begin{bmatrix} c & -c & 0 \\ -c & 2c & -c \\ 0 & -c & c \end{bmatrix} \begin{bmatrix} x_1 \\ x_2 \\ x_3 \end{bmatrix} + \begin{bmatrix} V'(x_1) \\ V'(x_2) \\ V'(x_3) \end{bmatrix} = \underbrace{\begin{bmatrix} F_{1,0} \sin(\Omega_0 t + \beta_0) \\ F_{2,1} \sin(\Omega_2 t + \beta_2) \\ F_{3,1} \sin(\Omega_3 t + \beta_3) \end{bmatrix}}_{=: \begin{bmatrix} F_1(t) \\ F_2(t) \\ F_3(t) \end{bmatrix}}. \tag{99}$$

Where $\Omega_0 \approx 1$ is a low frequency and Ω_2 and Ω_3 are high frequencies, exciting the inner vibrations modes of the chain. The new coordinates, i.e., the center of mass and relative displacements, are defined as follows

$$\begin{bmatrix} \eta \\ y_2 \\ y_3 \end{bmatrix} = \begin{bmatrix} \frac{1}{3} & \frac{1}{3} & \frac{1}{3} \\ -1 & 1 & 0 \\ 0 & -1 & 1 \end{bmatrix} \begin{bmatrix} x_1 \\ x_2 \\ x_3 \end{bmatrix}. \tag{100}$$

Thus, the differential equations in the new coordinates become

$$\ddot{\eta} + \frac{V'(\eta - \frac{2}{3}y_2 - \frac{1}{3}y_3) + V'(\eta + \frac{1}{3}y_2 - \frac{1}{3}y_3) + V'(\eta + \frac{1}{3}y_2 + \frac{2}{3}y_3)}{3} = \frac{\sum_{i=1}^{3} F_i(t)}{3}, \tag{101}$$

or compacter

$$\ddot{\eta} + \frac{\sum_{i=1}^{3} V'(\eta + z_i(t))}{3} = \frac{\sum_{i=1}^{3} F_i(t)}{3}, \tag{102}$$

with $z_i := x_i - \eta$. The equations describing the relative motions are given by

$$\begin{bmatrix} \ddot{y}_2 \\ \ddot{y}_3 \end{bmatrix} + \begin{bmatrix} 2k & -k \\ -k & 2k \end{bmatrix} \begin{bmatrix} \dot{y}_2 \\ \dot{y}_3 \end{bmatrix} + \begin{bmatrix} 2c & -c \\ -c & 2c \end{bmatrix} \begin{bmatrix} y_2 \\ y_3 \end{bmatrix} + \underbrace{\begin{bmatrix} V'(x_2) - V'(x_1) \\ V'(x_3) - V'(x_2) \end{bmatrix}}_{\text{negligible}} = \begin{bmatrix} F_2(t) \underbrace{-F_1(t)}_{\text{negligible}} \\ F_3(t) - F_2(t) \end{bmatrix}, \tag{103}$$

where in Eq. (103), the force of the potential and the low-frequency excitation can be neglected, being much smaller than the force of the springs. The remaining equation system is linear, and its Laplace transform is given by

$$\underbrace{\begin{bmatrix} s^2 + 2ks + 2c & -ks - c \\ -ks - c & s^2 + 2ks + 2c \end{bmatrix}}_{=: \mathbf{A}(s)} \begin{bmatrix} Y_2(s) \\ Y_3(s) \end{bmatrix} = \mathbf{F}(s), \tag{104}$$

where $\mathbf{F}(\mathbf{s})$ is the Fourier transform of the excitation. The inverse of the system matrix $\mathbf{A}(s)$ is given by

$$\mathbf{A}^{-1}(s) = \frac{1}{(s^2+ks+c)\,(s^2+3ks+3c)} \begin{bmatrix} s^2+2ks+2c & ks+c \\ ks+c & s^2+2ks+2c \end{bmatrix}. \tag{105}$$

To facilitate the calculations, let us define the functions

$$G_l(s) := s^2 + lks + lc \qquad \text{for } l \in \{1,2,3\}, \tag{106}$$

$$G_0(s) := ks + c. \tag{107}$$

The transfer function is obtained by inserting $s = j\omega$. Then, we can rewrite Eqs. (106-107) which we can also write as

$$G_l(j\omega) = lc - \omega^2 + j\omega lk = \sqrt{(lc-\omega^2)^2 + l^2k^2\omega^2}\exp\left(j\arctan\frac{lk\omega}{lc-\omega^2}\right), \tag{108}$$

$$G_0(j\omega) = c - j\omega k = \sqrt{c^2+k^2\omega^2}\exp\left(j\arctan\frac{k\omega}{c}\right), \tag{109}$$

thus, we can write

$$\mathbf{G}(j\omega) = \frac{1}{G_1(j\omega)G_3(j\omega)} \begin{bmatrix} G_2(j\omega) & G_0(j\omega) \\ G_0(j\omega) & G_2(j\omega) \end{bmatrix}. \tag{110}$$

Based on Eq. (60), resonant frequencies are to be found around the values

$$\omega_{1,\text{peak}} = \sqrt{c - \frac{k^2}{2}}, \tag{111}$$

$$\omega_{2,\text{peak}} = \sqrt{3\left(c - \frac{3k^2}{2}\right)}. \tag{112}$$

We now define the values of the high-frequency excitations as follows.

$$\Omega_2 = \omega_{2,\text{Peak}}, \tag{113}$$

$$\Omega_3 = \omega_{1,\text{Peak}}. \tag{114}$$

We can obtain the amplitude and phase of the stationary solutions corresponding to $F_2(t)$ by

$$\begin{bmatrix} Y_{2,2} \\ Y_{3,2} \end{bmatrix} = \frac{1}{G_1(j\Omega_2)G_3(j\Omega_2)} \begin{bmatrix} G_2(j\Omega_2) & G_0(j\Omega_2) \\ G_0(j\Omega_2) & G_2(j\Omega_2) \end{bmatrix} \begin{bmatrix} F_2e^{j\beta_2} \\ -F_2e^{j\beta_2} \end{bmatrix}. \tag{115}$$

Using the identity $G_2(j\omega) - G_0(j\omega) = G_1(j\omega)$ we can simplify Eq. (115) as follows.

$$\begin{bmatrix} Y_{2,2} \\ Y_{3,2} \end{bmatrix} = \frac{1}{G_3(j\Omega_2)} \begin{bmatrix} 1 \\ -1 \end{bmatrix} F_2 e^{j\beta_2}, \tag{116}$$

$$\begin{bmatrix} Y_{2,2} \\ Y_{3,2} \end{bmatrix} = \frac{2\sqrt{3}F_2}{9k\sqrt{4c-3k^2}} e^{j\left(\beta_2 - \arctan\left(\frac{\sqrt{12c-18k^2}}{3k}\right)\right)} \begin{bmatrix} 1 \\ -1 \end{bmatrix}, \tag{117}$$

where Eq. (117) is obtained by inserting Eq. (113) in Eq. (117).

Similarly, we can derive the stationary solution corresponding to $F_3(t)$. The results are as follows.

$$\begin{bmatrix} Y_{2,3} \\ Y_{3,3} \end{bmatrix} = \frac{1}{G_1(j\Omega_3)G_3(j\Omega_3)} \begin{bmatrix} G_0(j\Omega_3) \\ G_2(j\Omega_3) \end{bmatrix} F_3 e^{j\beta_3}. \tag{118}$$

Inserting Eq. (114) in Eq. (118) yields

$$\begin{bmatrix} Y_{2,3} \\ Y_{3,3} \end{bmatrix} = \frac{2F_2 e^{j(\beta_3 - \gamma_1 - \gamma_3)}}{k\sqrt{4c-k^2}\sqrt{16c^2+44ck^2-17k^4}} \begin{bmatrix} \sqrt{4c^2+4ck^2-2k^4}e^{j\gamma_0} \\ \sqrt{4c^2+20ck^2-7k^4}e^{j\gamma_2} \end{bmatrix}, \tag{119}$$

with

$$\gamma_0 := \arctan \angle G_0(j\omega_{1,\text{Peak}}) = \arctan\left(\frac{k\sqrt{4c-2k^2}}{2c}\right), \tag{120}$$

$$\gamma_l := \arctan \angle G_l(j\omega_{1,\text{Peak}}) = \arctan\left(\frac{lk\sqrt{4c-2k^2}}{(2l-2)\,c+k^2}\right) \quad \text{for } l \in \{1,2,3\}. \tag{121}$$

With the complex amplitudes $Y_{2,2} \ldots Y_{3,3}$ we can write the steady state solutions as

$$y_2(t) = |Y_{2,2}| \sin\left(\omega_{2,\text{Peak}} t + \angle Y_{2,2}\right) + |Y_{2,3}| \sin\left(\omega_{1,\text{Peak}} t + \angle Y_{2,3}\right), \tag{122}$$

$$y_3(t) = |Y_{3,2}| \sin\left(\omega_{2,\text{Peak}} t + \angle Y_{3,2}\right) + |Y_{3,3}| \sin\left(\omega_{1,\text{Peak}} t + \angle Y_{3,3}\right). \tag{123}$$

The particles' oscillations around their center of mass are given by

$$z_1(t) = -\frac{2}{3}y_2(t) - \frac{1}{3}y_3(t) = Z_{1,1}\sin(\omega_{1,\text{Peak}} t + \zeta_{1,1}) + Z_{1,2}\sin(\omega_{2,\text{Peak}} t + \zeta_{1,2}), \tag{124}$$

$$z_2(t) = \frac{1}{3}y_2(t) - \frac{1}{3}y_3(t) = Z_{2,1}\sin(\omega_{1,\text{Peak}} t + \zeta_{2,1}) + Z_{2,2}\sin(\omega_{2,\text{Peak}} t + \zeta_{2,2}), \tag{125}$$

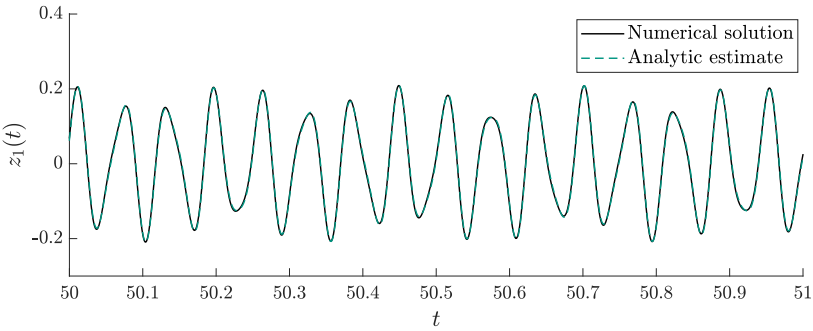

Fig. 5: Comparison of the numerical solution of $z_1(t)$ with the analytic one for $n = 3$, $m = 1$, $k = 3$, $c = 10000$, $F_0 = 0.33$, $F_2 = 200$, $F_3 = 100$, Ω_0=1, $\Omega_2 = \sqrt{3(c - \frac{3k^2}{2})}$, $\Omega_3 = \sqrt{c - \frac{k^2}{2}}$, $\beta_0 = \beta_2 = \beta_3 = \frac{\pi}{2}$

$$z_3(t) = \frac{1}{3}y_2(t) + \frac{2}{3}y_3(t) = Z_{3,1}\sin(\omega_{1,\mathrm{Peak}}t + \zeta_{3,1}) + Z_{3,2}\sin(\omega_{2,\mathrm{Peak}}t + \zeta_{3,2}), \tag{126}$$

where $Z_{1,1} \dots Z_{3,2}$ and $\zeta_{1,1} \dots \zeta_{3,2}$ are determined with the help of Eq. (70-72). Thus, the particle's vibrations around their center of mass are given by biharmonic functions, respectively. Since $\omega_{1,\mathrm{Peak}}$ and $\omega_{2,\mathrm{Peak}}$ are incommensurable, i.e., linearly independent over $\mathbb{Q}$, Theorem 1 can be applied to obtain the moments of the fast variable's CPD.

z_l with $l \in \{1, 2, 3\}$ is a biharmonic motion. In [27], the CPD of such functions was derived. For a function of the form $f(t) = A_1\sin(\omega_1 t+\beta_1)+A_2\sin(\omega_2 t+\beta_2)$ with ω_1 and ω_2 incommensurable and $A_1 \geq A_2$ (w.l.o.g.), the CPD is given by

$$\rho_{\mathrm{BH}}(x) = \begin{cases} 0 & \text{for } x < -A_1 - A_2, \\ \frac{1}{\pi^2\sqrt{A_1A_2}}K\left(\frac{(A_1+A_2)^2-x^2}{4A_1A_2}\right) & \text{for } -A_1 - A_2 < x < -A_1 + A_2, \\ \frac{2}{\pi^2\sqrt{(A_1+A_2)^2-x^2}}K\left(\frac{4A_1A_2}{(A_1+A_2)^2-x^2}\right) & \text{for } -A_1 + A_2 < x < A_1 - A_2, \\ \frac{1}{\pi^2\sqrt{A_1A_2}}K\left(\frac{(A_1+A_2)^2-x^2}{4A_1A_2}\right) & \text{for } A_1 - A_2 < x < A_1 + A_2, \\ 0 & \text{for } A_1 + A_2 < x, \end{cases} \tag{127}$$

where $K(\cdot)$ is the complete elliptic integral of the first kind. Eq. (127) is already too complicated for further calculations, but the first few moments of ρ_{BH} are easily calculated using Theorem 2 with $P = 2$, i.e.,

$$m_k = \left(\sum_{(\sum_{j=1}^{2} j_i)=k} \prod_{j=1}^{2} \frac{m_{j,j_i}}{j_i!}\right) k!, \tag{128}$$

where $m_{j,1}$ and $m_{j,2}$ are given by Eq. (94), respectively. The first few moments are

$$m_0 = 1, \tag{129}$$
$$m_1 = m_3 = m_5 = 0, \tag{130}$$
$$m_2 = \frac{A_1^2 + A_2^2}{2}, \tag{131}$$
$$m_4 = \frac{3}{8}A_1^4 + \frac{3}{2}A_1^2A_2^2 + \frac{3}{8}A_2^4. \tag{132}$$

Therefore, the corresponding moments of z_l are obtained by substituting A_1 and A_2 with $Z_{l,1}$ and $Z_{l,2}$, respectively.

Let us denote the averaged center of mass by $\xi = \langle \eta \rangle$. In Eq. (102) the only terms that are challenging to average are $V'(\eta + z_l(t))$ for $l \in \{1, 2, 3\}$. As shown by Eq. (83), for analytic functions $f(x)$, such as Eq. (98), averaging can be performed based on a series expansion. Using Eq. (83), the averages are calculated by

$$\langle V'(\eta + z_l(t)) \rangle = m_0 V'(\eta) + \underbrace{m_1}_{=0} V''(\eta) + \frac{m_2 V'''(\eta)}{2} + \underbrace{\dots}_{=0} \tag{133}$$
$$= (1 - 3m_2)\eta - \eta^3 \tag{134}$$
$$= \left(1 - 3\frac{Z_{1,l}^2 + Z_{2,l}^2}{2}\right)\eta - \eta^3, \tag{135}$$

where all the terms above m_4 disappear due to $V^{(k)}(x) = 0$ for $k \geq 4$. Inserting this result into Eq. (102) we find

$$\ddot{\xi} + \left(1 - \underbrace{\frac{\sum_{l=1}^{3} Z_{1,l}^2 + Z_{2,l}^2}{2}}_{=:d}\right)\xi - \xi^3 = \frac{F_{1,0}\sin(\Omega_0 t + \beta_0)}{3}, \tag{136}$$
$$\ddot{\xi} + \omega_d^2 \xi - \xi^3 = \frac{F_{1,0}\sin(\Omega_0 t + \beta_0)}{3}. \tag{137}$$

Here, d represents a detuning parameter influenced by all the underlying factors that contribute to the steady-state vibrations around the center of mass, denoted as $z_1(t), z_2(t)$, and $z_3(t)$. This equation mirrors a single particle's motion under harmonic excitation. However, the linear eigenfrequency of the system is detuned to $\omega_d = \sqrt{1 - d}$. Introducing appropriate dimensionless time and space coordinates

$$\tau := \omega_d t, \qquad \chi := \frac{\xi}{\omega_d}, \tag{138}$$

we obtain

$$\chi'' + \chi - \chi^3 = F\sin(\Omega\tau + \beta_0), \tag{139}$$

with

$$F := \frac{F_{1,0}}{3\omega_d^3}, \qquad \Omega := \frac{\Omega_0}{\omega_d}, \tag{140}$$

where $\square'$ denotes differentiation with respect to τ.

Eq. (146) has been widely investigated in the literature [37, 40–43] and, therefore, will not be further discussed in this article. However, in the next section, numerical simulations will be performed to compare the slow dynamics of the direct solution of Eq. (99) to the reduced system dynamics given by Eq. (146).

4.1 Numerical validation

In the following sections, we perform a comparative numerical simulation between the original 3 DoF model and the reduced 1 DoF model. The analysis calculates the escape time on a parameter region specified for Ω_0 and $F_{1,0}$. The parameter values used for the simulations are as follows: $n = 3$, $m = 1$, $k = 3$, $c = 10000$, $F_2 = 200$, $F_3 = 100$, $\Omega_2 = \sqrt{3(c - \frac{3k^2}{2})}$, $\Omega_3 = \sqrt{c - \frac{k^2}{2}}$, $\beta_0 = \beta_2 = \beta_3 = \frac{\pi}{2}$.

The model reduction yields the following results. The frequencies exciting the internal resonances are

$$\Omega_2 = 173.0881, \qquad \Omega_3 = 99.9775, \tag{141}$$

yielding to the complex amplitudes of the relative steady-state vibrations

$$Y_2 = \begin{bmatrix} 0.1283 + 0.0033j \\ -0.1283 - 0.0033j \end{bmatrix}, \qquad Y_3 = \begin{bmatrix} 0.1663 - 0.01j \\ 0.1668 + 0.005j \end{bmatrix}. \tag{142}$$

The vibrations around the center of mass are given by the complex amplitudes (including phase information) for Ω_2 and Ω_3 by

$$Z_1 = \begin{bmatrix} -0.0428 - 0.0011j \\ 0.0855 + 0.0022j \\ -0.0428 - 0.0011j \end{bmatrix}, \qquad Z_2 = \begin{bmatrix} -0.1664 + 0.005j \\ -0.0002 - 0.005i \\ 0.1666 + 0i \end{bmatrix}, \tag{143}$$

respectively. With these, we have

$$d = \frac{\sum_{l=1}^{3} |Z_{1,l}|^2 + |Z_{2,l}|^2}{2} = 0.0332, \tag{144}$$

$$\omega_d = \sqrt{1 - d} = 0.9832. \tag{145}$$

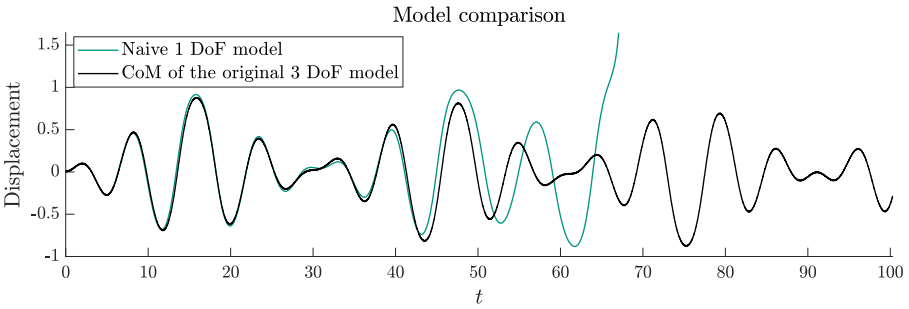

Fig. 6: Time evolution comparison between the original 3 DoF (cf. Eq. (99)) and the naive 1 DoF model without detuning parameter d for $F_0 = 0.33$ and $\Omega_0 = 1$ with homogeneous initial conditions. The remaining parameters are set as indicated in the main text. The discrepancies between the two models are salient

Thus, the reduced model becomes

$$\ddot{\xi}_1 + (1-d)\,\xi - \xi^3 = \frac{F_0}{3}, \tag{146}$$

$$\ddot{\xi}_1 + 0.9668\,\xi - \xi^3 = \frac{F_0}{3}. \tag{147}$$

Eq. (146) followed after a lengthy calculation to take into account the impact of the internal vibrations of the chain on the center of mass of the chain. One might approach the problem naively simply by neglecting the effect of internal vibrations. However, this primitive approach leads to incorrect results, which shall be demonstrated in Fig. 6 showing the time evolutions of the original 3 DoF (cf. Eq. (99)) and naively reduced system (cf. Eq. (146)) for $F_0 = 0.33$, $\Omega_0 = 1$ and homogeneous initial conditions. Indeed, Fig. 7 depicting the time evolutions of the original model and the averaging-based reduction shows a much better correspondence.

Using Melnikov analysis, it has been shown that escape from a quadratic-cubic potential may be preceded by chaotic motion [2, 5]. There is no compelling reason to believe that this would also not hold for a quadratic-quartic potential. Such a scenario, however, suggests the existence of a fractal boundary separating the escaping and non-escaping regimes. In this chaotic context, the system is susceptible to minor alterations in initial conditions or model errors. Consequently, the precise prediction of the escape time using a reduced model becomes infeasible within the chaotic region. However, the reduced model may yield accurate results in areas adjacent to this chaotic region. To test this hypothesis, we conducted a parameter study. The range for Ω_0 is set between 0.6 and 1.2, and for F_0, it is set between 0 and 1. Parallel to that, we also show how the averaging-based method performs compared to the naive method that neglects the internal vibrations of the chain. In Fig. 8, the escape times of the

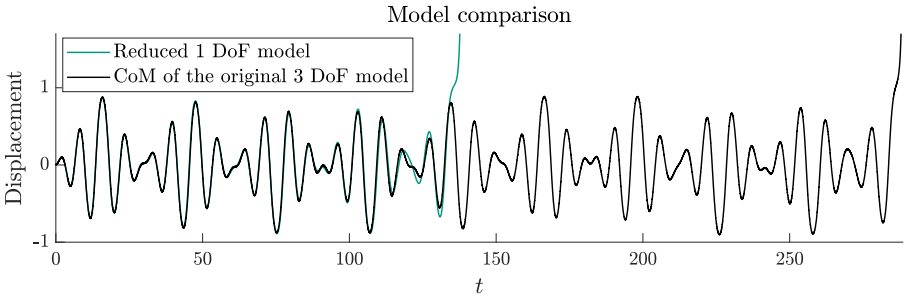

Fig. 7: Model validation: the original 3 DoF model (cf. Eq. (99)) and the reduced model with detuning parameter $d = 0.0332$ (cf. Eq. (146)) are compared. $F_0 = 0.33$, $\Omega_0 = 1$, and homogeneous initial conditions are chosen. The remaining parameters are specified in the main text. A good correspondence is observed between the two models; however, due to chaotic dynamics, they diverge over time. The reduced model accurately predicts the chain's escape, although not the exact escape time

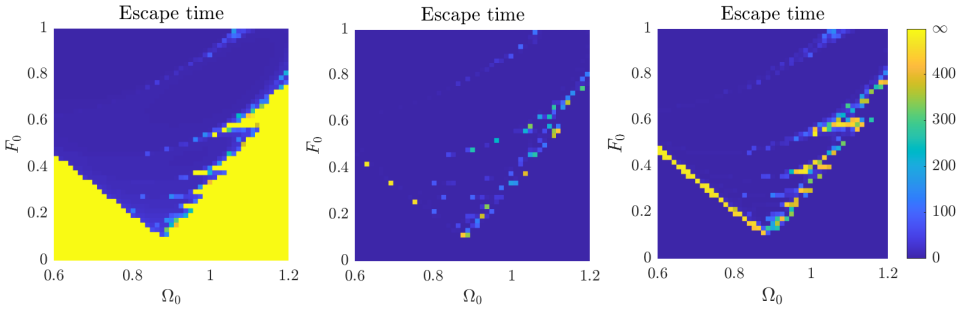

(a) Original model (b) $|t_{\mathrm{Esc,Orig}} - t_{\mathrm{Esc,Red}}|$ (c) $|t_{\mathrm{Esc,Orig}} - t_{\mathrm{Esc,Naive}}|$

Fig. 8: Model validation: panel (a) represents the escape times of the original system, varying the parameters F_0 and Ω_0 with homogeneous initial conditions applied. Panel (b) shows the absolute error in escape times of the reduced system relative to the original, using a detuning parameter of $d = 0.0332$. In contrast, panel (c) shows the naive model reduction approach that neglects the impact of internal vibrations corresponding to $d = 0$. The naive approach shows a notable shift in the frequency and force amplitude of the V-shaped escape boundary (cf. Eq. (140)), while the reduced model based on averaging agrees well with the original. Parameters not specified here adhere to those delineated in the main text

original model (cf. Fig. 8a), together with the absolute errors of the averaging-based reduction method (cf. Fig. 8b) and the naive reduction method (8c) are presented, respectively. Naive reduction results in a noticeable shift in the V-shaped escape boundary, indicating that neglecting internal vibrations leads to an inaccurate reduced model. The V-boundary shift occurs along the frequency and force axes, as predicted by Eq. (140).

The reduced model we derived is no longer stiff, which markedly improved computational efficiency and significantly decreased simulation time in our executed example. Specifically, the computational cost was reduced by 99.75%, which corroborates the effectiveness of the model reduction technique.

5 Discussion

This paper presented a model reduction approach for an externally excited, strongly coupled n-particle chain in a potential well. The reduction method leverages the different frequency scales between the chain's quick internal vibrations and the slow movements of its center of mass within the potential well. The choice of excitation is notably flexible; a polyharmonic excitation affecting all particles is acceptable as long as it includes only one low frequency. This feature ensures that the remaining frequencies primarily trigger high-frequency internal vibrations of the chain.

In addition to the strong coupling between the particles, it is also assumed that non-small damping forces exist among them. This results in the rapid decay of high-frequency transient motions. Such a setting permits a straightforward analytical calculation of steady-state fast vibrations, assuming that the forces from the potential are negligible compared to the linear spring forces. Consequently, the fast relative motions become known time-dependent functions in the nonlinear differential equation governing the motion of the chain's center of mass. The net effect of these fast oscillations on the CoM's differential equation can be accurately approximated by averaging.

A theorem is introduced that extends the cross-correlation-based averaging technique [27] to scenarios where polyharmonic fast motions are present, provided the frequencies are linearly independent over $\mathbb{Q}$. A second theorem outlines how to calculate the moments of the CPD for such composite motions, which is especially useful for averaging a polynomial function. Building on these findings, we derive the effective potential, resulting in a reduced system with one degree of freedom.

As an illustrative example, a chain of three particles in a quadratic-quartic potential well, excited by a triharmonic force, is presented. The model reduction is carried out analytically, and numerical validation is performed by computing the escape time for both models across various excitation force and frequency values. In the case of the chosen quadratic-quartic potential, the impact of high-frequency excitation manifests solely as a detuning of the potential's linearized natural frequency, which allows for the use of several analytical methods already available in the literature.

6 Conclusions and scope for future research

The model reduction offers two main advantages. First, it enables us to grasp the fundamental slow dynamics of the system and identify the underlying slow

force field. Second, the computational cost is significantly reduced. The simple example involving three particles achieved a simulation time reduction of 99.75%. Importantly, as the number of particles increases and their interactions become stronger, making the differential equation system stiffer, the benefits of model reduction become increasingly pronounced.

Future research could extend in several directions. First, the model reduction techniques could be applied to more complex potential wells beyond polynomial forms to test the range of applicability of the current methods. Second, other types of excitation, such as stochastic or time-dependent forces, could be incorporated to see how they affect both slow dynamics and computational efficiency.

Also worth exploring is how the model scales with more particles and complex interaction mechanisms. In particular, quantifying the computational advantages would be informative in stiff systems. In line with the observed 99.75% time reduction in the three-particle example, a scaling law could be developed for computational time savings in larger systems.

Extending the model reduction to 2- and 3-dimensional potentials could also be a valuable line of inquiry, providing insights into more physically realistic systems.

A separate area of focus could be investigating cases where there is no damping between the particles. This aspect is fascinating because it would influence the model's effectiveness and accuracy, given that no advantage can be gained from the decay of fast transients.

A further extension could involve examining particle chains with nonlinear couplings, a plausible generalization, to ascertain how such complexities influence the system's slow and fast dynamics.

Acknowledgments

This work was funded by the Deutsche Forschungsgemeinschaft (DFG, German Research Foundation) - Project number: 508244284. This support is greatly appreciated.

In preparing this paper, the language was improved using the ChatGPT 4.0 model. This enhancement is on par with the language correction services typically offered by academic journals.

Declarations

The authors have nothing to declare.

Conflict of interest

The authors declare that they have no conflict of interest.

Data availability

This manuscript does not have associated data.

References

[1] Landau, L.D., Lifshitz, E.M.: Mechanics, 3rd edn. Butterworth, Oxford (1976)

[2] Thompson, J.M.T.: Chaotic phenomena triggering the escape from a potential well. Engineering Applications of Dynamics of Chaos, CISM Courses and Lectures **139**, 279–309 (1991)

[3] Virgin, L.N., Plaut, R.H., Cheng, C.-C.: Prediction of escape from a potential well under harmonic excitation. International Journal of Non-Linear Mechanics **27**(3), 357–365 (1992). https://doi.org/10.1016/0020-7462(92)90005-R

[4] Virgin, L.N.: Approximate criterion for capsize based on deterministic dynamics. Dynamics and Stability of Systems **4**(1), 56–70 (1989) https://arxiv.org/abs/https://doi.org/10.1080/02681118908806062. https://doi.org/10.1080/02681118908806062

[5] Sanjuan, M.A.F.: The effect of nonlinear damping on the universal escape oscillator. Int. J. Bifurc. Chaos **9**, 735–744 (1999)

[6] Kramers, H.A.: Brownian motion in a field of force and the diffusion model of chemical reactions. Physica **7**(4), 284–304 (1940). https://doi.org/10.1016/S0031-8914(40)90098-2

[7] Fleming, G.R., Hänggi, P.: Activated Barrier Crossing. Default Book Series. University of Chicago and University of Augsburg, Singapore (1993)

[8] Antonio Barone, G.P.: Physics and Applications of the Josephson Effect. John Wiley and Sons, Ltd, Address unknown (1982). https://doi.org/10.1002/352760278X.fmatter. https://onlinelibrary.wiley.com/doi/abs/10.1002/352760278X.fmatter

[9] Elata, D., Bamberger, H.: On the dynamic pull-in of electrostatic actuators with multiple degrees of freedom and multiple voltage sources. Journal of Microelectromechanical Systems **15**, 131–140 (2006). https://doi.org/10.1109/JMEMS.2005.864148

[10] Leus, V., Elata, D.: On the dynamic response of electrostatic mems switches. Journal of Microelectromechanical Systems **17**, 236–243 (2008). https://doi.org/10.1109/JMEMS.2007.908752

[11] Younis, M., Abdel-Rahman, E., Nayfeh, A.: A reduced-order model for electrically actuated microbeam-based mems. Journal of Microelectromechanical Systems **12**, 672–680 (2003). https://doi.org/10.1109/JMEMS.2003.818069

[12] Alsaleem, F., Younis, M., Ruzziconi, L.: An experimental and theoretical investigation of dynamic pull-in in mems resonators actuated electrostatically. Journal of Microelectromechanical Systems **19**, 794–806 (2010). https://doi.org/10.1109/JMEMS.2010.2047846

[13] Ruzziconi, L., Younis, M.I., Lenci, S.: An electrically actuated imperfect microbeam: Dynamical integrity for interpreting and predicting the device response. Meccanica **48**(7), 1761–1775 (2013). https://doi.org/10.1007/s11012-013-9707-x

[14] Zhang, W.-M., Yan, H., Peng, Z.-K., Meng, G.: Electrostatic pull-in instability in mems/nems: A review. Sensors and Actuators A: Physical **214**, 187–218 (2014). https://doi.org/10.1016/j.sna.2014.04.025

[15] Mann, B.P.: Energy criterion for potential well escapes in a bistable magnetic pendulum. Journal of Sound and Vibration **323**(3), 864–876 (2009). https://doi.org/10.1016/j.jsv.2009.01.012

[16] Arnold, V., Kozlov, V., Neishtadt, A.: Mathematical aspects of classical and celestial mechanics. transl. from the russian by a. iacob. 2nd printing of the 2nd ed. 1993. Itogi Nauki i Tekhniki Seriia Sovremennye Problemy Matematiki (1985)

[17] Quinn, D.D.: Transition to escape in a system of coupled oscillators. International Journal of Non-Linear Mechanics **32**(6), 1193–1206 (1997). https://doi.org/10.1016/S0020-7462(96)00138-2

[18] Belenky, V.L.: Stability and Safety of Ships—Risk of Capsizing. The Society of Naval Architects and Marine Engineers, Jersey City (2007)

[19] Talkner, P., Hanggi, P.: New Trends in Kramers' Reaction Rate Theory. Springer, Berlin (1995)

[20] Gendelman, O.V.: Escape of a harmonically forced particle from an infinite-range potential well: a transient resonance. Nonlinear Dynamics **93**(1), 79–88 (2018). https://doi.org/10.1007/s11071-017-3801-x

[21] Rega, G., Lenci, S.: Dynamical integrity and control of nonlinear mechanical oscillators. Journal of Vibration and Control **14**, 159–179 (2008). https://doi.org/10.1177/1077546307079403

[22] Orlando, D., Gonçalves, P., Lenci, S., Rega, G.: Influence of the mechanics

of escape on the instability of von mises truss and its control. Procedia Engineering **199**, 778–783 (2017). https://doi.org/10.1016/j.proeng.2017.09.048

[23] Habib, G.: Dynamical integrity assessment of stable equilibria: a new rapid iterative procedure. Nonlinear Dynamics **106**(3), 2073–2096 (2021). https://doi.org/10.1007/s11071-021-06936-9

[24] Karmi, G., Kravetc, P., Gendelman, O.: Analytic exploration of safe basins in a benchmark problem of forced escape. Nonlinear Dynamics **106**, 1–17 (2021). https://doi.org/10.1007/s11071-021-06942-x

[25] Genda, A., Fidlin, A., Gendelman, O.: Safe basins of escape of a weakly-damped particle from a truncated quadratic potential well under harmonic excitation (2022). https://doi.org/10.21203/rs.3.rs-2239131/v1

[26] Genda, A., Fidlin, A., Gendelman, O.: On the escape of a resonantly excited couple of particles from a potential well. Nonlinear Dynamics **104**(1), 91–102 (2021). https://doi.org/10.1007/s11071-021-06312-7

[27] Genda, A., Fidlin, A., Gendelman, O.: Cross-correlation and averaging: An equivalence based on the classical probability density. Technical report (2023). https://doi.org/10.5445/IR/1000163303

[28] Fidlin, A., Drozdetskaya, O.: On the averaging in strongly damped systems: The general approach and its application to asymptotic analysis of the sommerfeld effect. Procedia IUTAM **19**, 43–52 (2016). https://doi.org/10.1016/j.piutam.2016.03.008. IUTAM Symposium Analytical Methods in Nonlinear Dynamics

[29] Fidlin, A., Juel Thomsen, J.: Non-trivial effects of high-frequency excitation for strongly damped mechanical systems. International Journal of Non-Linear Mechanics **43**(7), 569–578 (2008). https://doi.org/10.1016/j.ijnonlinmec.2008.02.002

[30] Noschese, S., Pasquini, L., Reichel, L.: Tridiagonal toeplitz matrices: properties and novel applications. Numerical Linear Algebra with Applications **20**(2), 302–326 (2013) https://arxiv.org/abs/https://onlinelibrary.wiley.com/doi/pdf/10.1002/nla.1811. https://doi.org/10.1002/nla.1811

[31] Robinett, R.W.: Quantum and classical probability distributions for position and momentum. American Journal of Physics **63**(9), 823–832 (1995) https://arxiv.org/abs/https://pubs.aip.org/aapt/ajp/article-pdf/63/9/823/12163222/823_1_online.pdf. https://doi.org/10.1119/1.17807

[32] DeGroot, M.H.: Probability and Statistics, (1986)

[33] Weyl, H.: Über die gleichverteilung von zahlen mod. eins. Mathematische Annalen **77**(3), 313–352 (1916). https://doi.org/10.1007/BF01475864

[34] Cornfeld, I., Fomin, S., Sinai, Y.: Ergodic Theory. Grundlehren der mathematischen Wissenschaften, vol. 245, p. 486. Springer, New York (1982)

[35] Petrov, V.V.: Sums of Independent Random Variables, 1st edn. Ergebnisse der Mathematik und ihrer Grenzgebiete. 2. Folge, p. 348. Springer, Berlin, Heidelberg (1975). https://doi.org/10.1007/978-3-642-65809-9. Softcover ISBN: 978-3-642-65811-2, Published: 22 October 2011; eBook ISBN: 978-3-642-65809-9, Published: 06 December 2012. https://doi.org/10.1007/978-3-642-65809-9

[36] Bulmer, M.G.: Principles of Statistics, New edn. Dover Books on Mathematics. Dover Publications Inc., New York (1979). Originally published in 1965

[37] Gendelman, O.V., Karmi, G.: Basic mechanisms of escape of a harmonically forced classical particle from a potential well. Nonlinear Dynamics **98**(4), 2775–2792 (2019). https://doi.org/10.1007/s11071-019-04985-9

[38] Kravetc, P., Gendelman, O.: Approximation of potential function in the problem of forced escape. Journal of Sound and Vibration **526**, 116765 (2022)

[39] Karmi, G., Kravetc, P., Gendelman, O.: Analytic exploration of safe basins in a benchmark problem of forced escape. Nonlinear Dynamics **106**, 1573–1589 (2021)

[40] Kravetc, P., Gendelman, O.: Approximation of potential function in the problem of forced escape. Journal of Sound and Vibration **526**, 116765 (2022). https://doi.org/10.1016/j.jsv.2022.116765

[41] Kravetc, P., Gendelman, O., Fidlin, A.: Resonant escape induced by a finite time harmonic excitation. Chaos: An Interdisciplinary Journal of Nonlinear Science **33**(6), 063116 (2023) https://arxiv.org/abs/https://pubs.aip.org/aip/cha/article-pdf/doi/10.1063/5.0142761/17960760/063116_1_5.0142761.pdf. https://doi.org/10.1063/5.0142761

[42] Karmi, G., Kravetc, P., Gendelman, O.: Analytic exploration of safe basins in a benchmark problem of forced escape. Nonlinear Dynamics **106**(3), 1573–1589 (2021). https://doi.org/10.1007/s11071-021-06942-x

[43] Karmi, G.: Analytic Exploration of Safe Basins in a Benchmark Problem of Forced Escape (2022). https://www.graduate.technion.ac.il/Theses/Abstracts.asp?Id=33683